OPTICAL ROTATION CURVES OF DISTANT GALAXIES : KINEMATICS AND EVOLUTION OUT TO z ~1

N. P. VOGT & A. C. PHILLIPS
UCO / Lick Observatory, UCSC, Santa Cruz, CA, 95064-1077, USA

High resolution *HST* images have been combined with Keck 10m telescope spectra to study the internal kinematics of 16 faint disk galaxies in the redshift range 0.1 $\lesssim z \lesssim$ 1. These data form a high redshift Tully-Fisher relation that spans three magnitudes and extends to well below L^*, with no obvious change in shape or slope with respect to the local Tully–Fisher relation. The small offset of 0.4 B mag is attributed to luminosity evolution in the field galaxy population, and does not correlate with galaxy mass. A comparison of disk surface brightness between local and high redshift samples yields a similar offset of 0.6 B mag. These results provide further evidence for only a modest increase in luminosity with lookback time for this population.

Galaxy evolution models range from those with mild amounts of luminosity brightening in the past (Gronwall & Koo 1995) to those requiring more dramatic changes (Glazebrook *et al.* 1995) to explain the large numbers of faint blue galaxies. A direct measure of luminosity evolution in field galaxies will help to distinguish between various hypotheses. The correlation between rotational velocity (mass) and luminosity of disk galaxies (the "Tully–Fisher relation") provides a powerful tool with which to study distant galaxies and to investigate their evolution. With detailed kinematic information we can derive the fundamental parameter of mass and use it to directly trace the luminosity evolution for specific classes of galaxies.

Sixteen inclined disk galaxies with *HST WFPC2* images from the flanking fields of the *Hubble Deep Field* and other regions (providing V and I photometry, disk and bulge deconvolutions, and galaxy type, orientation, and inclination) have been observed with the Low Resolution Imaging Spectrograph (LRIS) on the Keck 10m telescope. Object selection was based on the following criteria: (*i*) undistorted disk morphology; (*ii*) inclination greater than 30°; (*iii*) no interacting companions or obscuring foreground stars; and (*iv*) $I_{814} \leq 22.5$. The selection was made with no apriori knowledge of redshifts or intrinsic luminosities. Spatially resolved major axis velocity profiles have been acquired using a 600 line mm^{-1} grating (1.26 Å and 0.″215 per pixel) for emission lines ranging from Hα through [O II] λ3727. Gaussian profiles were fit to these rotation curves, and an exponential disk model with flat terminal velocity was used to deconvolve the effects of slit width and position angle, galaxy inclination, and seeing to derive a maximum circular velocity for each galaxy from the observed rotation curve.

The shapes of the rotation curves of these high redshift galaxies are similar to those of local galaxies in both form and amplitude, and, when combined with the apparent disks in the *HST* images, show conclusively that there were massive disks in place at $z \sim 1$ in some galaxies. The rotation curves are traceable to ~3 exponential scale lengths (R_d) in the disks, a length comparable to the extent of rotation curves for local galaxies (*cf.,* Vogt 1995), and the maximum velocities are comparable to those of local spirals. Rough calculations yield masses between 1 and 5 $\times$ 10^{11} $M_\odot$, well within the range of masses found for nearby spiral galaxies.

The kinematics of these distant galaxies show evidence for only a modest increase in luminosity of $\Delta M_B \lesssim 0.4$ compared to Tully–Fisher relations for local galaxies. This offset represents an *upper limit* to luminosity evolution of these field galaxies, as any magnitude-limited sample is biased towards more luminous objects; our analysis is restricted to objects with detectable emission lines – actively star-forming galaxies which are likely to have elevated B luminosities; some terminal velocities are lower limits; and we may be overcorrecting for extinction if galaxies were less dusty at earlier epochs. The *Hubble Deep Field* data extend the luminosity range of our total sample to $-21.8 \lesssim M_B \lesssim -19$. *There is no deviation from a linear relation over this range*, *i.e.,* there is no evidence in these data for different amounts of luminosity evolution in different luminosity or mass regimes.

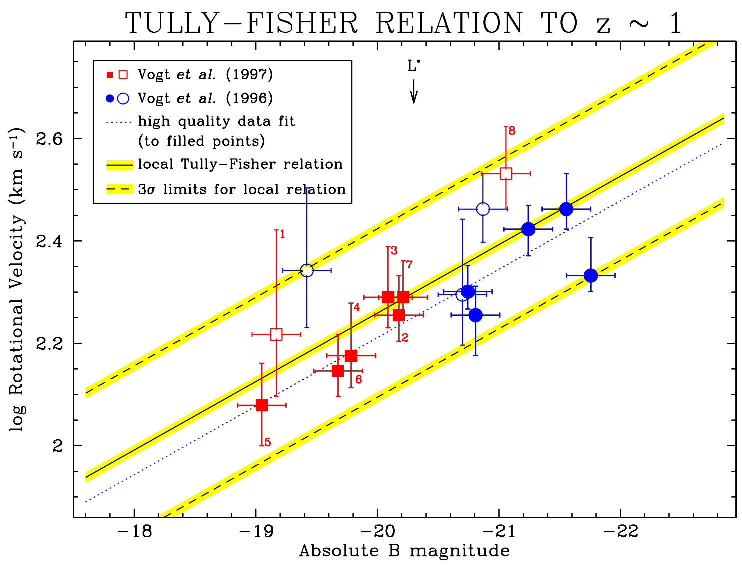

Figure 1: Tully–Fisher diagram: eight recently observed galaxies (squares, numbered in increasing redshift for identification on Fig. (3) from the *HDF* region and eight galaxies (circles) taken from Vogt *et al.* (1996) are compared to the Pierce & Tully (1992) relationship based on H I velocity width measurements for a set of cluster spirals; highest quality points are solid. Velocities have been corrected by $\sin i$ and the magnitudes corrected for internal extinction. The best-fit B-band relation (solid line) and 3σ limits (dashed lines) from Pierce & Tully are shown. The weighted fit to the 11 highest quality Tully–Fisher galaxies (dotted line; assuming the same slope) produces an offset of 0.36 ± 0.13 mag. The *HDF* data extends this trend for a set of sub-L* galaxies. We adopt $H_0 = 75$ km s^{-1} Mpc^{-1} and $q_0 = 0$.

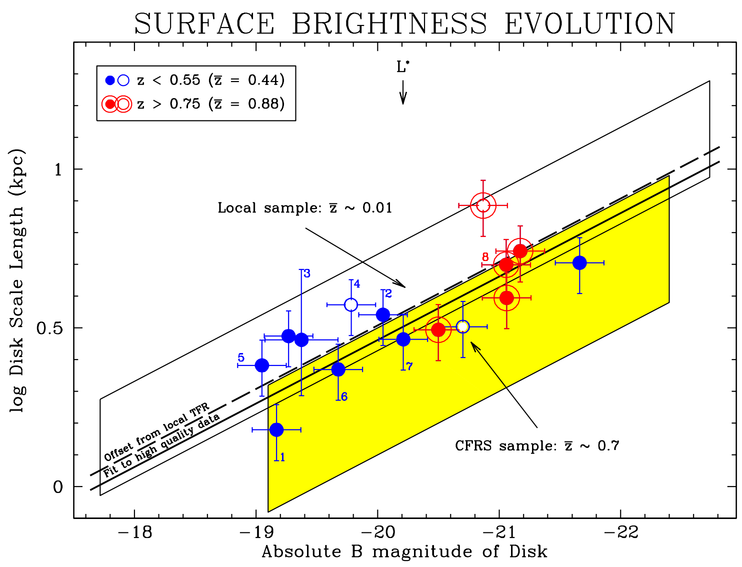

Figure 2: Disk surface brightness evolution diagram: exponential disk scale lengths are plotted vs. disk B luminosity for the 15 disk galaxies in the sample (*HDF* galaxies are again numbered in increasing redshift, and a double nucleus source from Vogt *et al.* 1996 is excluded). Open symbols denote disks with apparent inclination $i \geq 80°$, which may suffer from large systematic errors. The solid line is the offset (0.59 ± 0.13 mag) found by a weighted fit to the 12 disks with inclination angles less than 80°, while the dashed line indicates the luminosity offset (0.36 ± 0.13 mag) found with respect to the local TF relation. The two techniques are in good agreement. The five sources with redshift $0.75 \leq z \leq 1$ are circled. The region occupied by local spirals (from de Jong 1995) is white; that populated by the galaxies at redshift $\bar{z} \sim 0.7$ from Schade *et al.* (1996) is lightly shaded. The median offset in our high redshift data is significantly less than that seen in the Schade *et al.* sample, implying that the selection criteria for the two samples differ.

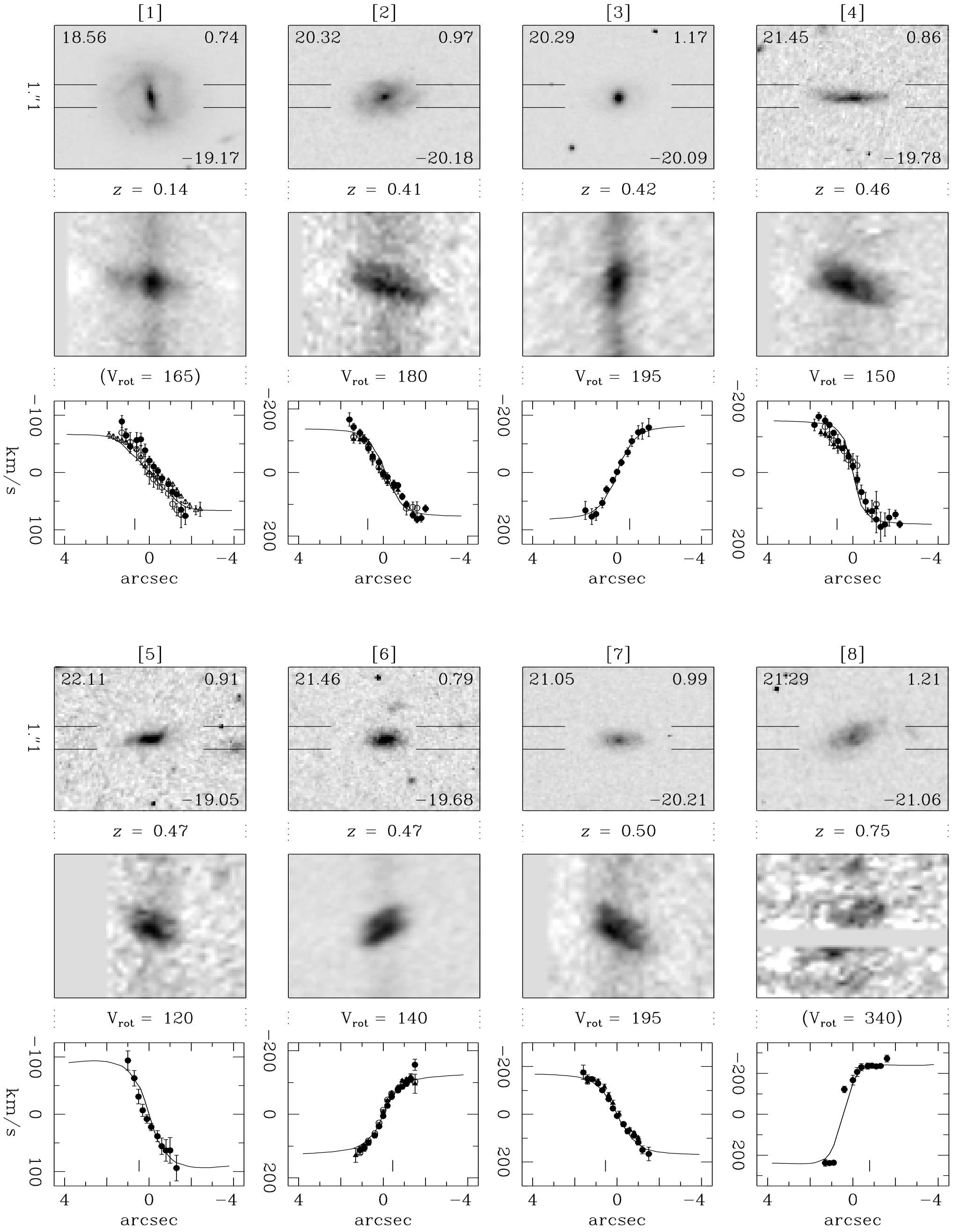

Figure 3: HDF Tully–Fisher spirals and their velocity curves: scales are identical and spatial axes aligned for each set of three plots. The WFPC2 I-band image of each galaxy is shown (*top*), along with its I_{814}, V_{606}–I_{814}, and M_B magnitudes and the LRIS slit width and orientation. Below is a ∼40Å section of the LRIS spectrum centered around the redshifted [O II] λ3727 doublet (*middle*). In the velocity plots (*bottom*), points represent the observed velocities: [O II] (●), Hβ (filled △), [O III] λ5007 (○), and Hα (unfilled △). Error bars are internal errors from the line-fitting technique. Data are shown only where the S/N was adequate; the Hβ and [O III] lines are not fit for several sources because of weak line strength, interference caused by night-sky OH emission lines, or fringing in the red portion of the spectrum. The solid line is the fit to the model emission line(s), and the intrinsic circular velocity of the model is noted (parentheses indicate lower-quality sources). A small tick marks the measured disk scale length. *Individual notes:* (1) all emission lines plus [N II] λ6583 were traced (only three are shown for legibility), but the strong bar and face-on nature of this galaxy make this a poor candidate; (2) measured [O II] velocities are somewhat larger than [O III] and Hβ, so the median velocity at each radius was fit; (3) early-type ring galaxy with [O II] flux concentrated in core, [O III] and Hβ too weak to trace; (5) [O III], Hβ too weak to trace; (6) note good agreement between [O II] and both [O III] and Hβ, observed with different gratings; (7) note excellent agreement of Hβ and [O II]; (8) night sky line bisects [O II] emission, leading to large uncertainties.

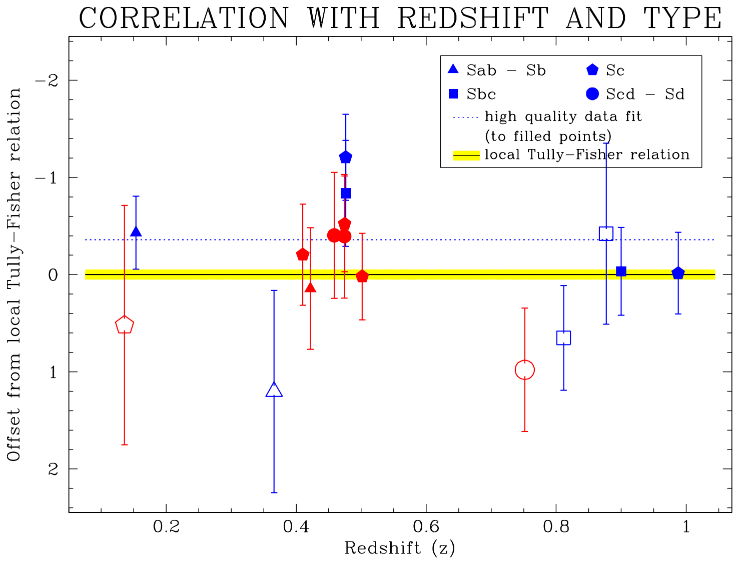

Figure 4: Tully–Fisher offset diagram: brightening relative to the Pierce and Tully (1992) local Tully–Fisher relationship is shown as a function of galaxy redshift and type, with the weighted fit to the 11 highest quality Tully–Fisher candidate galaxies from Fig. 1 (dotted line). There is no notable increase in brightening as a function of redshift for this sample, nor is there a clear trend with type.

We also calculate offsets from local surface brightness relations, allowing comparison of the two techniques for evaluating evolution of a population of galaxies. The apparent brightening at the high mass end could be caused by a bias toward higher-than-average luminosities among the most distant objects, as well as by luminosity evolution. We find our sample to have an overall offset of 0.6 mag with respect to local galaxies, in good agreement with the offset of 0.4 mag in the Tully–Fisher relation.

Acknowledgments

The authors thank the UCSC members of the DEEP project for their assistance in these endeavors. Funding was provided by the Center for Particle Astrophysics; NSF grants AST-9529098, AST-922540, and AST-9120005; NASA grants AR-06337.08-94A, AR-06337.21-94A, GO-05994.01-94A, AR-5801.01-94A, and AR-6402.01-95A.

References

1. R. S. de Jong, Ph. D. thesis, University of Groningen, 1995
2. K. Glazebrook, R. Ellis, B. Santiago, & R. Griffiths, MNRAS, 275, L19, 1995.
3. C. Gronwall & D. C. Koo, ApJ, 440, L1, 1995.
4. M. J. Pierce & R. B. Tully, ApJ, 387, 47, 1992.
5. D. Schade., R. G. Carlberg, H. K. C. Yee, O. López-Cruz, & E. Ellingson, ApJ, 465, L103, 1996.
6. N. P. Vogt, T. Herter, M. P. Haynes, & S. Courteau, ApJ, 415, L95, 1993.
7. N. P. Vogt, Ph. D. thesis, Cornell University, 1995
8. N. P. Vogt, D. A. Forbes, A. C. Phillips, C. Gronwall, S. M. Faber, G. D. Illingworth, & D. C. Koo, ApJ, 465, L15, 1996.
9. N. P. Vogt, A. C. Phillips, S. M. Faber, J. Gallego, C. Gronwall, R. Guzmán, G. D. Illingworth, D. C. Koo, & J. D. Lowenthal, ApJ, 479, L121, 1997.